Low Turn-on Field of ZnO Nanostructures Grown with Catalyst-Free Vapor-Phase Transport

Su-Hua Yang, Ming-Wei Tsai, Li-Li Chang, Po-Jui Chiang

Department of Electronic Engineering, National Kaohsiung University of Applied Sciences
Kaohsiung 807, Taiwan, R.O.C., shya@kuas.edu.tw

ABSTRACT

ZnO nanostructures were synthesized with catalyst-free process on a ZnO seed layer by the vapor-phase trasnport. The aspect ratio of nanostructures varied with growth conditions because of different growth rates at axial and radial directions. A high aspect ratio of 50.7 was obtained when nanostructures were grown with a ZnO/C weight ratio of 4:6 at 1000°C for 2 h. Surface morphology of nanostructures was not changed by the doping of Ga, however, growths on the (100) and (101) planes were facilitated, which led to variations in luminescence and field emission properties of electrons. The ZnO:Ga nanostructures with a low turn-on electric field of 0.57 V/μm was achieved. The optimum Ga doping concentration was 0.5 at%.

Keywords: pseudo-catalyst, seed layer, field emission

1 INTRODUCTION

ZnO nanostructures have attracted a great deal of attention because they have a variety of possible applications in optoelectronic related devices [1–6], especially for field-emission lightings (FELs). FEL is a well-known illumination technology, which composes of a field-emitter cathode and a phosphor screen anode. Usually, field-emitter with a low resistivity, high aspect ratio, and large emission area is preferred for high emission efficiency of electrons.

However, the growth and morphology of ZnO nanostructures are varied with the growth conditions, such as source composition, dopant substance, ambience, growth temperature and time. Accordingly, for the growth of ZnO nanostructures by the vapor-phase transport, two issues are concerned: nucleation sites and self-assembly [7–9].

In this study, ZnO nanostructures were synthesized by vapor-phase transport, the influences of growth conditions on the characteristics of nanostructures were discussed in detail. In addition, the variations of cathodoluminescence (CL) and field emission ability of electrons of ZnO nanostructures by the addition of Ga atoms were analysed.

2 EXPERIMENTAL PROCEDURE

A p-type (100) silicon wafer was used as the substrate for the growth of ZnO nanostructures. ZnO seed layer, 100 nm-thick, was deposited by a RF magnetron sputtering to speed up the synthesis of ZnO nanostructures.

ZnO and graphite powders were used as the source materials, they were mixed and then put on a boat. Subsequently, the boat was loaded in the central hot zone of a horizontal furnace. Afterward, ZnO nanostructures were grown under Ar/O_2 atmosphere. Furthermore, Ga_2O_3 with Ga concentration of 0, 0.5, and 1 at% was doped. Growth temperatures were ranged in 900–1050°C; and growth time was 30–50 min.

The crystal structures of nanostrucutres were investigated by X-ray diffraction (XRD) using Cu K_α radiation and a nickel filter. Surface morphologies were evaluated by a field-emission scanning electron microscope (HR-SEM). CL analyses were performed by JEOL 6330.

Moreover, field emission characteristics were carried out under a pressure of 5×10^{-6} torr. Current and voltage characteristics were simultaneously measured by a Keithley 2410 SourceMeter.

3 RESULTS AND DISCUSSION

The morphology of nanostructures is varied with the growth conditions significantly. Nanostructures were rod-, needle- and thin-film shapes at 950, 1000, and 1050°C, respectively. ZnO/C weight ratio increased over 2/3, aspect ratio and growth rate were decreased. Furthermore, diameter and length of nanostructures increased with the growth time. Table 1 shows the aspect ratios of ZnO nanostructures grown with different conditions.

Growth condition		Aspect ratio
Temperature (°C)	900	1.135
	950	6.605
	1000	27.461
	1050	4.98
Weight ratio ZnO/C	3/7	32.7
	2/3	50.7
	1	27.3
	3/2	2.69
Growth time (min)	30	27.3
	40	40.4
	50	15.2

Table 1: Aspect ratios of ZnO nanostructures grown with different conditions.

XRD patterns shows that ZnO:Ga nanostructures were developed along the [002] direction and was grown perpendicularly to the substrate surface. Crystalline direction of nanostructures was unchanged even if Ga atoms were doped, as shown in Fig. 1. Meanwhile, no diffraction peaks corresponding to impurity phases were found. The lattice parameters of *a* and *c* of ZnO:Ga, analyzed from XRD, were 0.3249 and 0.5206 nm, respectively. However, growths on the (100) and (101) planes were enhanced with the increase in Ga doping concentration. Obviously, growth orientation of ZnO nanostructures was altered by the doping of Ga atoms, and the luminescence properties and electron emission efficiency were varied accordingly.

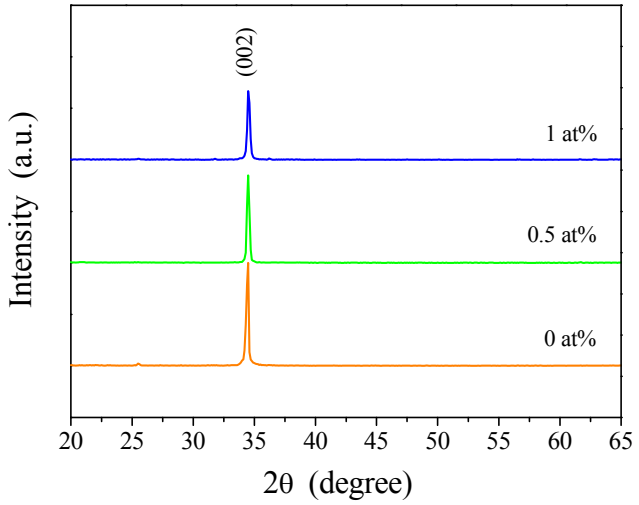

Figure 1: XRD patterns of ZnO:Ga with different Ga doping concentrations.

The high resolution TEM (HRTEM) image of ZnO nanostructure is shown in Fig. 2(a). Obviously, the nanostructure was grown along the [002] direction with a lattice spacing approximately of 0.52 nm, which is consistent with the result in XRD pattern. The selected area electron diffraction (SAED) pattern of ZnO nanostructure is displayed in Fig. 2(b). It shows single-crystalline wurtzite structure of ZnO nanostructures was grown.

Figure 2(c) shows a SEM image of ZnO:Ga nanostructures for Ga concentration of 0.5 at%. Surface morphology of nanostructures was not changed even though Ga atoms were doped. This is attributed to the configuration-limiting ability of Ga, because Zn atom is more active than the Ga atom in chemical property. Zn-terminated (001) surface enriched with Zn atoms, as a result, fast growth of ZnO nanostructure along the longitudinal direction by self-catalyst process is proceeded. The doping concentration of Ga^{3+} ions in ZnO:Ga nanostructures was 0.24 at% when 0.5 at% of Ga atoms in the souce materials was used. Figure 3 shows the EDS spectrum of ZnO:Ga nanostructures.

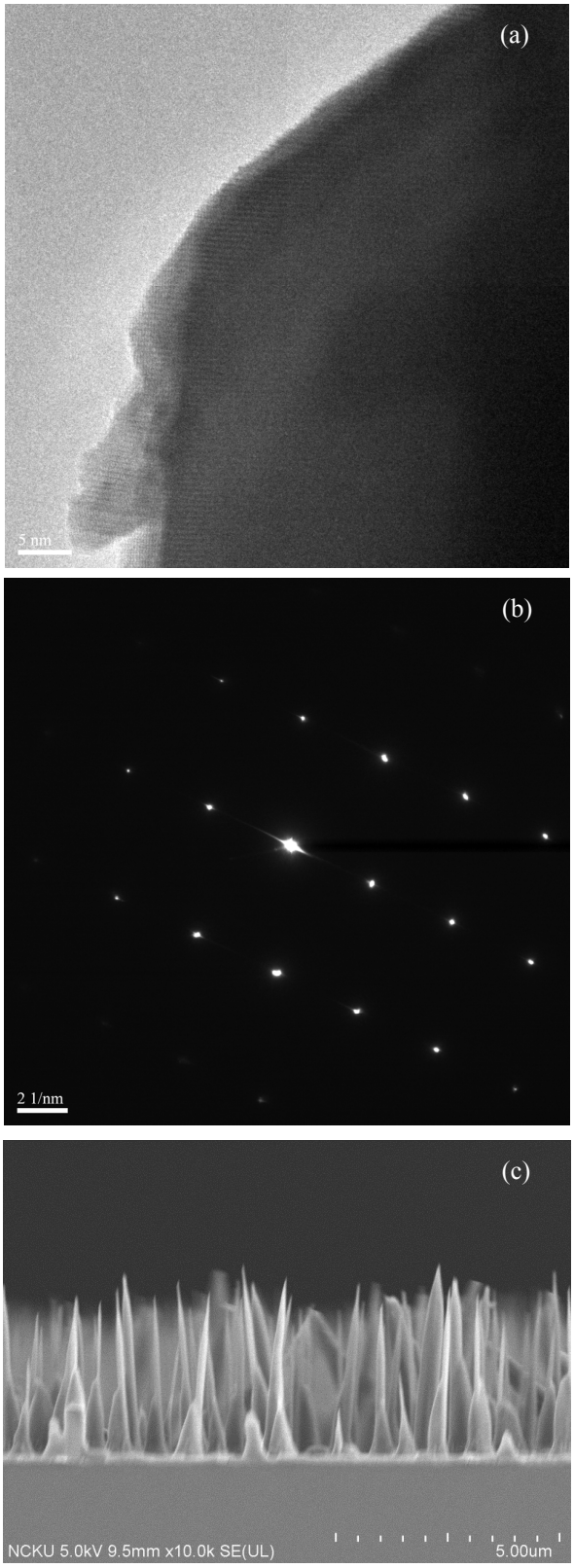

Figure 2: (a) HRTEM and (b) SAED images of ZnO nanostructure; (c) SEM image of ZnO:Ga nanostructures.

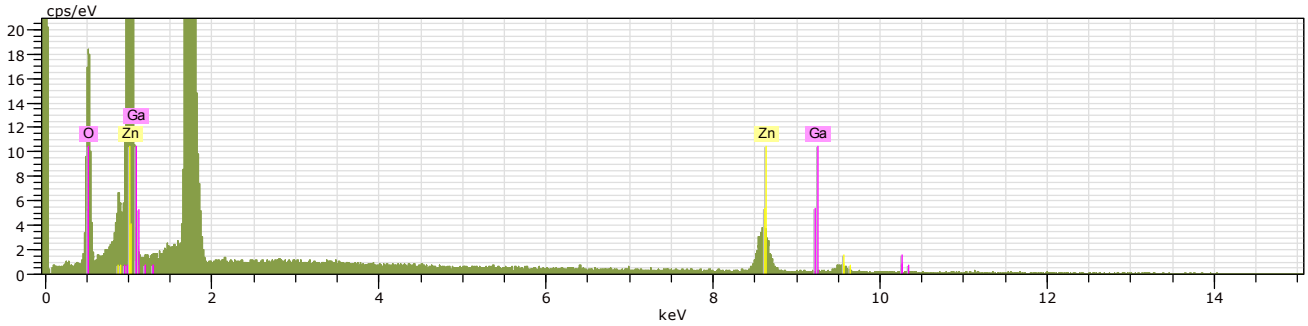

Figure 3: EDS spectrum of ZnO:Ga nanostructures.

Table 2 lists the atomic ratios of O, Zn, and Ga when 0.5 and 1 at% of Ga atoms in source were doped. The substitution of Ga^{3+} to Zn^{2+} ions introduced a large number of electrons, which led to an increase in conductivity of the nanostructures. However, crystallinity of nanostructures was decayed and an increased resistivity of nanostructures was resulted when a high Ga concentration was doped.

Atom	Atomic ratio	
	0.5 at%	1 at%
O	59.37	63.04
Zn	40.39	36.61
Ga	0.24	0.36

Table 2: Atomic ratios of O, Zn, and Ga in ZnO:Ga when 0.5 and 1 at% Ga in source materials were used.

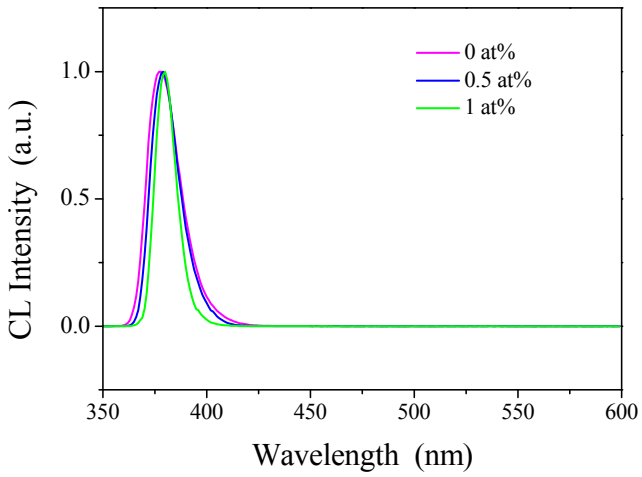

Figure 4: CL spectra of ZnO:Ga nanostructures with different Ga doping concentrations.

Figure 4 is CL spectra of ZnO:Ga nanostructures. The good crystallinity of nanostructures showed a strong and sharp near band edge (NBE) emission and no defect-related visible-light emission. Slightly red shift, from wavelength of 377, 379, to 380 nm, was observed when Ga doping concentration was increased from 0, 0.5, to 1 at%, respectively. Meanwhile, when Ga ions were doped, a decreased NBE emission was observed. This is compatible with the result of XRD measurements.

Field emission characteristics of ZnO:Ga nanostructures are shown in Fig. 5, where nanostructures were grown at Ga concentrations of 0, 0.5, and 1 at%. The turn-on electric field (E_{on}) was defined when the emission current density was reached 10 μA/cm^2. In Fig. 5, the E_{on} were 1.04, 0.57, and 0.91 V/μm for ZnO nanostructures grown with 0, 0.5, and 1 at% of Ga, respectively; the corresponding field enhancement factors (β) were 2457, 2563 and 2479, which were calculated from the slopes of the Fowler-Nordheim plots with a ZnO work function of 5.3 eV. The highest current density of 2.02 mA/cm^2 was obtained when ZnO:Ga nanostructures were doped with 0.5 at% of Ga atoms.

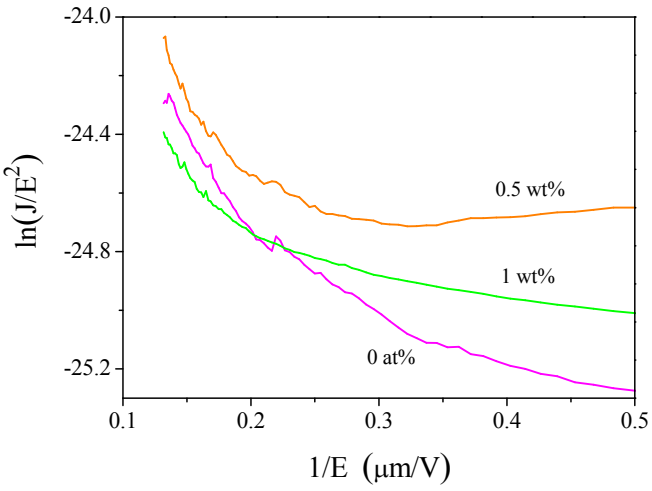

Figure 5: Field emission characteristics of ZnO:Ga nanostructures grown with different Ga doping concentrations.

Table 3 lists the E_{on} and β values for the ZnO:Ga nanostructures doped with 0, 0.5, and 1 at% of Ga atoms. It shows that when 0.5 at% Ga atoms was doped, the lowest E_{on} of 0.57 V/μm and the highest β of 2563 were obtained. Clearly, the conductivity of nanostructures was improved by Ga doping. High stable current density was obtained when a constant voltage of 900 V was applied continuously for 5 hours.

Parameter	Doping concentration		
	0 at%	0.5 at%	1 at%
E_{on} (V/μm)	1.04	0.57	0.91
β	2457	2563	2479

Table 3: Turn-on electric field and field enhancement factor for ZnO:Ga nanostructures doped with 0, 0.5 and 1 at% of Ga atoms.

4 CONCLUSIONS

In this study, a 100 nm-thick ZnO film was deposited on Si substrate, which was used as seed layer for ZnO nanostructures grown with catalyst-free vapor-phase transport. When ZnO/C weight ratio was 4:6, nanostructures with a faster growth rate and high aspect ratio of 50.7 (diameter 68.7 nm and length 3.48 μm) were grown. The preferred growth plane of nanostructures was unchanged, still on (002) plane, even if Ga atoms were doped. Surface morphology of nanostructures was not changed as Ga was doped, although their lengths became longer.

Ga doping facilitated electron transport to the nanostructures surface, consequently, the lowest E_{on} of 0.57 V/μm and the highest β of 2563 were obtained.

ACKNOWLEDGEMENT

The authors would like to thank the Ministry of Science and Technology of the Republic of China, Taiwan, for financially supporting this research under contract No. MOST 103-2221-E-151-008.

REFERENCES

[1] G. Kenanakis, N. Katsarakis, J. Environ. Chem. Eng. 2, 1416–1422, 2014.
[2] H. Nguyen, C. T. Quy, N. D. Hoa, N. T. L., Nguyen V. Duy, V. V. Quang, N. V. Hieu, Sens. Actuators, B, 193, 888–894, 2014.
[3] Y. Abdi, S. M. Jebreiil Khadem, P. Afzali, Curr. Appl. Phys., 14, 227–231, 2014.
[4] Z. Xu, C. Zhang, W. Wang, Y. Bando, X. Bai, D. Golberg, Nano Energy, 13, 233–239, 2015.
[5] Z. Han, J. Li, W. He, S. Li, Z. Li, J. Chu, Y. Chen, Microelectron. Eng., 111, 199–203, 2013.
[6] I. Udom, Y. Zhang, M. K. Rama, E. K. Stefanakos, A. F. Hepp, R. Elzein, R. Schlaf, D. Y. Goswami, Thin Solid Films, 564, 258–63, 2014.
[7] Y. Ji, Mater. Lett., 138, 92–95, 2015.
[8] J.-C. Wang, Y.-T. Liang, F.-C. Cheng, C.-H. Fang, H.-I. Chen, C.-Y. Tsai, J.-A. Jiang, T.-E. Nee, J. Lumin., 136, 11–16, 2013.
[9] V. Khranovskyy, M. O. Eriksson, G. Z. Radnoczi, A. Khalid, H. Zhang, P. O. Holtz, L. Hultman, R. Yakimova, Physica B, 439, 50–53, 2014.